Phase diagram and high-resolution photoemission study of the superconducting and magnetic pseudoternary body-centered-tetragonal $Ho(Rh_{1-x}Ru_x)_4B_4$ system

R. Knauf, A. Thomä, and H. Adrian
Physikalisches Institut der Universität Erlangen–Nürnberg, Erwin-Rommel-Strasse 1, D-8520 Erlangen, Federal Republic of Germany

R. L. Johnson
Max-Planck-Institut für Festkörperforschung, Heisenbergstrasse 1, D-7000 Stuttgart 80, Federal Republic of Germany
(Received 5 August 1983)

The phase diagram for the body-centered-tetragonal superconducting pseudoternary system $Ho(Rh_{1-x}Ru_x)_4B_4$ ($0.07 \leq x \leq 1$) is reported for temperatures above 1.3 K, revealing an abrupt drop in the superconducting critical temperature T_c near the critical concentration $x_{cr} \approx 0.40$, which is characteristic for this class of compounds. In order to clarify the origin of this phenomenon, synchrotron radiation from the DORIS storage ring (Hamburg, Germany) has been used to measure high-resolution photoemission spectra for samples with $x = 0.07$, 0.37, and 0.90. The analysis of the valence-band data near the Fermi energy E_F shows a shift of E_F to lower energies with increasing x relative to the transition-metal d-electron structure. The results are consistent with existing band-structure calculations for the primitive-tetragonal modification of this structure type and provide a straightforward explanation of the observed T_c behavior.

I. INTRODUCTION

The discovery of superconductivity and magnetism in the ternary compound families (for a review, see Ref. 1) RMo_6X_8 (X = S,Se) (Refs. 2 and 3) and RRh_4B_4,[4,5] where the magnetic rare-earth ions R are situated at a regular sublattice, provided new experimental possibilities to study the interplay between these two ordering phenomena. In 1977, Johnston found a body-centered-tetragonal modification, now known as the $LuRu_4B_4$ type, of the earlier reported primitive-tetragonal RRh_4B_4 phase ($CeCo_4B_4$ type) by substituting a few atomic percent of Ru for Rh.[6] The essential difference between the two structures is manifested in the orientation of every second $(Rh_{1-x}Ru_x)_4B_4$ tetrahedra.

In the $LuRu_4B_4$-type compound series $R(Rh_{0.85}Ru_{0.15})_4B_4$ superconductivity was observed for R = Pr, Eu, Dy, Ho, Er, Tm, Lu, and also Y, whereas the isomorphic series RRu_4B_4 orders ferromagnetically for R = Nd, Gd, Tb, Dy, Ho, and Er.[6] The different behavior of the Rh- and Ru-rich compounds allows the influence of the occupation of the transition-metal sublattice on the interactions between superconductivity and magnetism to be studied. So far, pseudoternary phase diagrams of $R(Rh_{1-x}Ru_x)_4B_4$ have been reported for R = Er,[7] Dy,[8] and Y.[9–11] They reveal the common interesting feature that the superconducting transition temperature T_c remains nearly constant with increasing x up to $x \approx 0.3$, however, this value may depend on the heat treatment of the samples.[11] With further increasing x, T_c was found to drop below 1 K in a small interval $\Delta x \approx 0.1$. For $x = 1$ only the nonmagnetic compounds with Y (Refs. 9 and 11) and Lu (Ref. 6) are superconducting. This abrupt drop in T_c is remarkable because it occurs in systems with magnetic ions and in nonmagnetic systems. Furthermore, it can be observed when the concentration of valence electrons is changed (Ru for Rh), but also when it remains constant (Ir for Rh).[12–14] In the vicinity of the critical concentration the character of the magnetic ordering appears to change from antiferromagnetism in coexistence with superconductivity to ferromagnetism.[8] Hitherto the reasons for these extremely unusual superconducting and magnetic properties were not clear. In earlier work to explain the abrupt drop in T_c, concentrating on KVV boron Auger transitions[11] and some additional ultraviolet photoemission spectroscopy (UPS) and x-ray photoemission spectroscopy data,[15] no abrupt change in charge transfer, electronic structure, or lattice parameters has been found.[10]

In order to contribute to the clarification of this peculiar phenomenon we prepared samples of the pseudoternary system $Ho(Rh_{1-x}Ru_x)_4B_4$ and measured the ac susceptibility and high-resolution photoelectron spectra. The motivation for this work was to search for stoichiometry-dependent properties of the band structure which could explain the drastic decrease in T_c. Special attention was focused on the electronic density of states $N(E)$ near the Fermi energy E_F, which is of fundamental importance for superconductivity as well as magnetic exchange interaction. As there are no band-structure calculations available for the $LuRu_4B_4$-type structure, the experimental results are compared with calculations performed for the $CeCo_4B_4$-type structure.[16] However, we believe it is reasonable to assume that the difference in the orientation of the tetrahedra does not lead to significant changes in $N(E)$, as the main contribution to the density of states near E_F originates from the transition-metal (T) d electrons which are strongly localized at the T_4B_4 clusters.

II. EXPERIMENTAL

The samples were prepared by arc-melting in a zircon-gettered argon atmosphere. First the [Rh]/[Ru] ratio was fixed by melting stochiometric amounts of rhodium and

ruthenium ingots together. Then appropriate pieces of boron and holmium were successively melted in. The ingots were remelted several times to improve homogeneity. In this way we obtained nearly spherical samples of about 1 g. Mass losses during arc-melting were about 1 wt.%. The x-ray-diffraction patterns from pulverized pieces of our samples can be indexed with the body-centered-tetragonal structure reported by Johnston.[6] We also observe small amounts of RhB and in some cases one or two additional impurity lines. The superconducting, and as far as observable, magnetic ordering temperatures, were determined by ac-susceptibility measurements using a standard mutual-inductance bridge (27.4 Hz) in a ^{4}He-bath cryostat with a lowest attainable temperature of 1.3 K. Pieces cut from the original ingots with $x=0.07$, 0.37, and 0.90 were used for photoemission measurements. In addition to the data presented in this paper, magnetization, specific-heat, and resistivity measurements have been started with cylindrical parts of the samples and will be reported elsewhere after completion.

The photoemission spectra were obtained using an ultrahigh-vacuum system with a base pressure of 1×10^{-10} Torr. The measurements were performed in a double-pass cylindrical mirror analyzer (PHI) at a fixed pass energy of 15 eV. Synchrotron radiation from the DORIS storage ring in Hamburg was employed, monochromatized by a high-resolution grating monochromator. Spectra were recorded at a photon-energy range of 21.6—168 eV. The total experimental resolution of the system was determined by measuring the molybdenum Fermi edge, and found to be 0.25 and 0.33 eV at $h\nu=21.6$ and 60 eV, respectively.

Before each run, the sample surfaces were cleaned by scraping *in situ* with a diamond file. This method was preferred to cleaning by ion bombardment in order to avoid any changes in surface composition.

III. RESULTS

A. Phase diagram

The phase diagram of $Ho(Rh_{1-x}Ru_x)_4B_4$ (Fig. 1) shows the general behavior described above. T_c remains nearly constant at 6.3 K from $x=0.07$ up to $x=0.30$, and then drops within a small range of concentration ($\Delta x<0.10$) below 1.3 K. Below T_c we observe no reentrant behavior except for the sample with nominal composition, $x=0.40$. This sample shows the onset of a superconducting phase transition which is still incomplete at 1.4 K, where superconductivity is destroyed by the onset of magnetic order. Our method is not sensitive to the antiferromagnetic transitions reported by Muto *et al.*[17,18] Preliminary evaluations of magnetization and resistive H_{c2} measurements for cylinders with $x\leq0.37$ reveal strong evidence for antiferromagnetic order with Néel temperatures T_N below 1.5 K in coexistence with superconductivity. For high ruthenium concentrations ($x\geq0.90$) we observe magnetic order, probably ferromagnetism. The superconducting transition widths are in the range 150—180 mK for $x<0.30$ and increase up to 600 mK for $x=0.35$. Figure 1 clearly shows

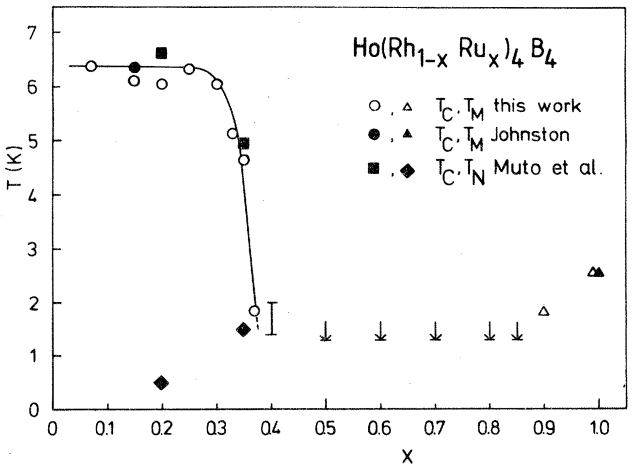

FIG. 1. Superconducting and magnetic ordering temperatures vs ruthenium concentration x for $Ho(Rh_{1-x}Ru_x)_4B_4$. The arrows indicate that no superconducting or magnetic transition was observed down to 1.3 K. The error bar indicates a superconducting transition which is not complete and is destroyed by magnetic order. The line is drawn as a guide to the eye.

that superconducting and magnetic properties strongly depend on the ruthenium concentration x, although the concentration of magnetic moments is not varied at all.

B. Photoemission spectra

A typical valence-band spectrum of $Ho(Rh_{1-x}Ru_x)_4B_4$ for $x=0.37$ and photon energy $h\nu=60$ eV is presented in Fig. 2. The binding energy is referred to the Fermi level E_F. The three characteristic peaks labeled $A-C$ in Fig. 2 and a shoulder S near E_F can be distinguished. These three peaks are common features of all the measured samples. However, there is a significant dependence of the position of peak A on the ruthenium content of the compound. In Table I the binding energies E_B of peaks $A-C$ for the different samples are listed relative to E_F.

A set of valence-band spectra ($x=0.37$) for different photon energies from $h\nu=40.8-168$ eV is shown in

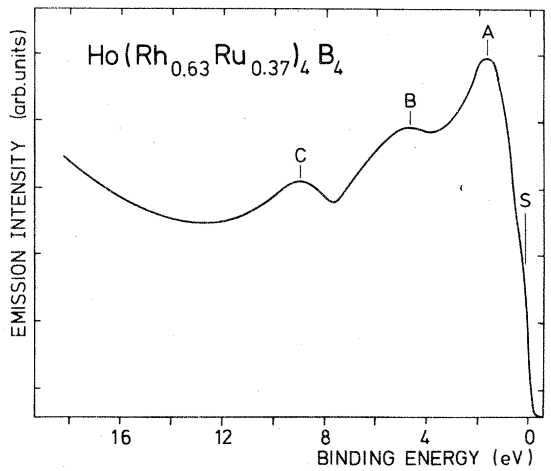

FIG. 2. Valence-band spectrum of $Ho(Rh_{0.63}Ru_{0.37})_4B_4$ excited at $h\nu=60$ eV.

TABLE I. Binding energies E_B (in eV) of valence-band features in $Ho(Rh_{1-x}Ru_x)_4B_4$ relative to the Fermi level E_F ($h\nu=60$ eV).

Peak	A	B	C
E_B ($x=0.07$)	1.8±0.1	4.8±0.1	8.9±0.1
E_B ($x=0.37$)	1.6±0.1	4.7±0.1	8.9±0.1
E_B ($x=0.90$)	1.2±0.1	4.8±0.1	8.9±0.1

Fig. 3. All spectra are aligned with respect to E_F. Because of the low photon flux at high photon energies caused by the transmission characteristics of the monochromator the analyzer resolution had to be increased so that the total resolution for the spectrum recorded at $h\nu=168$ eV was about 1 eV. There is a distinct maximum of intensity at $h\nu=60$ eV comparing peak A to peaks B and C, which themselves show only little variation of their relative intensities up to photon energies of $h\nu=80$ eV. However, if the photon energy exceeds $h\nu=80$ eV, the spectra indicate a strong decrease of peak A, accompanied by a steady increase of peak C relative to peak B. This behavior was found for all the samples in the same way and will be discussed in detail in the following section.

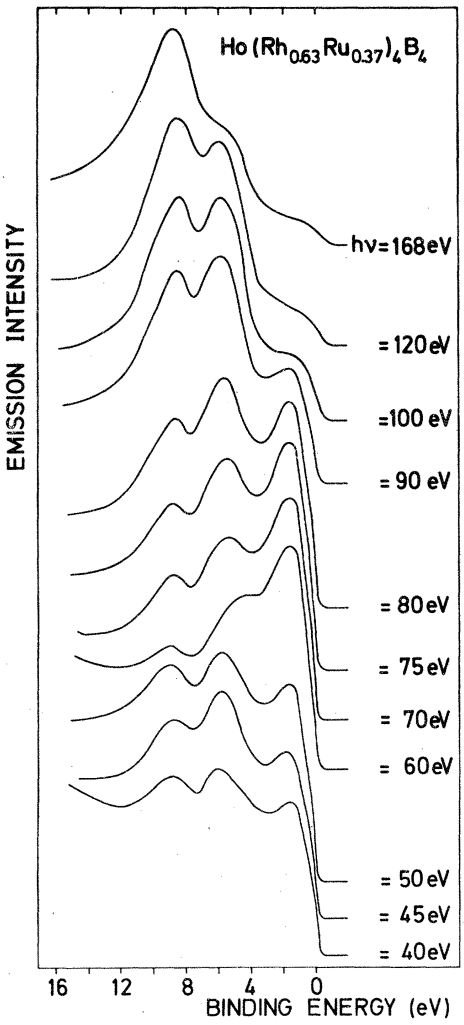

FIG. 3. Set of valence-band spectra of $Ho(Rh_{0.63}Ru_{0.37})_4B_4$ for different photon energies $h\nu$.

IV. DISCUSSION

The main advantage of using synchrotron radiation over standard UPS methods is the possibility to change the photon energy continuously and to measure the energy dependence of the photoionization cross sections or resonant photoemission mechanisms.[19] The different behavior of particular features in the spectra allows conclusions about the character of the corresponding parts of the band structure and electronic state to be drawn.

Figure 4 shows the valence-band spectra of pure-Ho metal for various photon energies measured by Gerken,[20] which reveal essentially two dominant peaks corresponding to the $4f$ states. Upon varying the photon energy, the most striking effect is the resonance behavior around $h\nu=170$ eV. The reason for this well-understood phenomenon is the onset of resonant photoemission at the $4d\rightarrow 4f$ threshold in this range of photon energies, as the binding energy E_B ($4d$) is about 160 eV.[21] If one normalizes the spectra for equal height of the largest peak, this leads to a strong reduction of the peak close to E_F. For the system $Ho(Rh_{1-x}Ru_x)_4B_4$ we find exactly the same behavior for the features indexed B and C. From this analogy and because of the measured binding energies, which are close to the values in the pure element ($E_B=8.6$ and 5.2 eV from Ref. 21), we conclude that peak B and

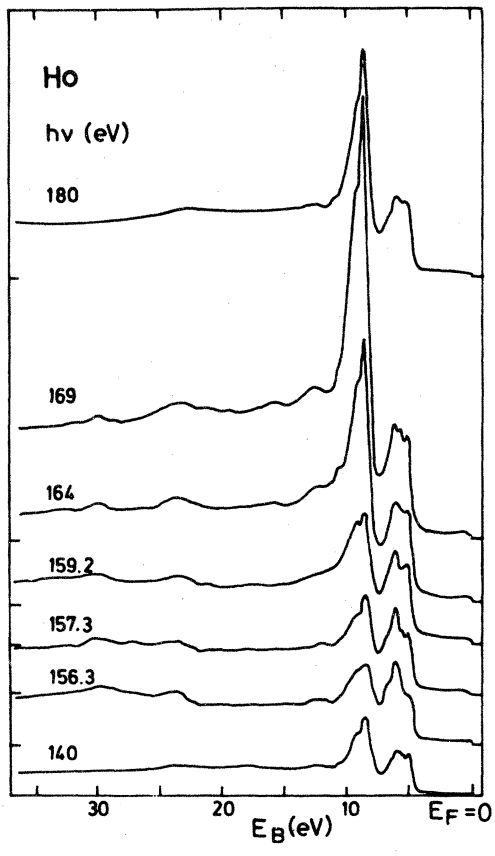

FIG. 4. Valence-band spectra of pure Ho for different photon energies $h\nu$ near the $4d\rightarrow 4f$ threshold (total experimental resolution $\Delta E=0.3$ eV) (from Ref. 20).

especially C mainly result from the $4f$ electrons of Ho. Significant boron s and p states as shown in UPS measurements ($h\nu=21.6$ eV) of $Y(Rh_{1-x}Ru_x)_4B_4$ in Ref. 15 are estimated to have only a small contribution to our spectra, because of a comparatively low density of states at the boron sites[16,22] in conjunction with a very low cross section for higher photon energies. In addition, spectra measured with $h\nu=60$ eV of the binary compound RhB where peak C is totally absent support this peak identification.

Feature A of the spectra is assigned to the d electrons of the transition metals Rh and Ru. The photon-energy dependence of feature A in Fig. 3 agrees very well with optical-absorption measurements[23] reported earlier which support this interpretation. This is further corroborated by band-structure calculations[22] of the $CeCo_4B_4$-type $HoRh_4B_4$, which show that the contribution of Rh d electrons is dominant near E_F (see Fig. 5). Another important result of the band-structure calculations is that E_F is situated in an isolated narrow peak in $N(E)$ formed by d electrons, which is separated from the main structure by a narrow range ($\Delta E=0.3$ eV) of a low density of states. Owing to the limited experimental resolution, this detail is smeared out and only causes a shoulder (S) which can be clearly identified in the spectra obtained with Rh-rich samples (see Fig. 2).

If one assumed rigid bands, a substitution of Ru for Rh reduces the total number of d electrons, and therefore shifts E_F to lower energies. In the case of the critical concentration $x_{cr}=0.40$ the number of d electrons is reduced by about 1.6 states/formula unit which approximately corresponds to a shift of E_F into the energy range with low $N(E)$. Using the total and l-decomposed partial density of states, we estimate the shift of E_F to about 0.23 and 0.41 eV, respectively.

In order to compare in detail the parts of our spectra close to E_F for samples with different Ru content, we took additional narrow scans with low statistical errors for $h\nu=60$ eV. These are shown normalized and aligned to the position of feature A in Fig. 6(a). The clearly observable shift of the shoulder agrees reasonably well with the change of E_F as outlined above for the substitution of Ru for Rh. This is also demonstrated in Fig. 6(b) which shows the partial d-electron density of states of Fig. 5 broadened by a Gaussian function with $\sigma=0.3$ eV representing the total experimental resolution. The different curves have been obtained by shifting E_F as indicated. As the calculated $N(E_F)$ is only given for discrete values of E in units of 0.01 Ry=0.136 eV (histogram bars), a shift of E_F is only reasonable in multiples of this unit. The values ΔE_F given in Fig. 6(b) which correspond to two and five histogram bars are chosen to obtain the

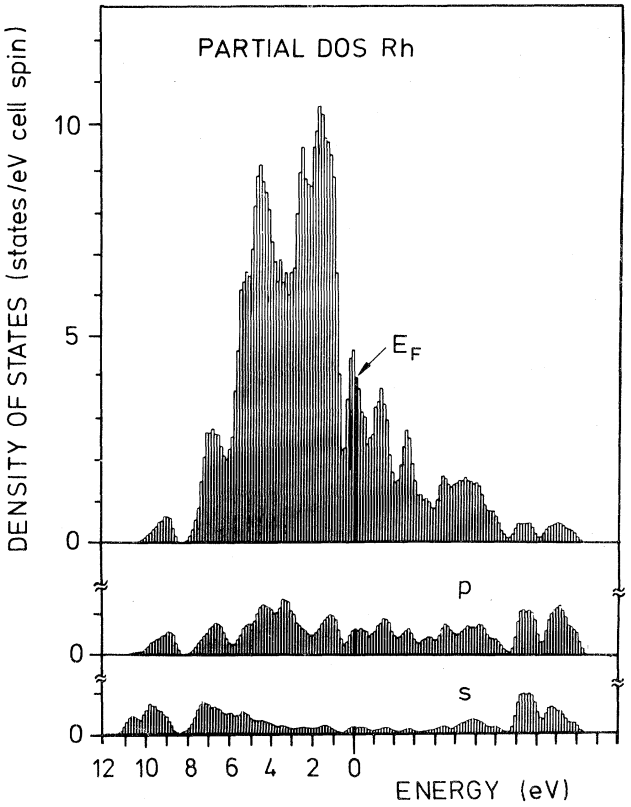

FIG. 5. Calculated l-decomposed partial density of states (DOS) for Rh in $HoRh_4B_4$ (from Ref. 22).

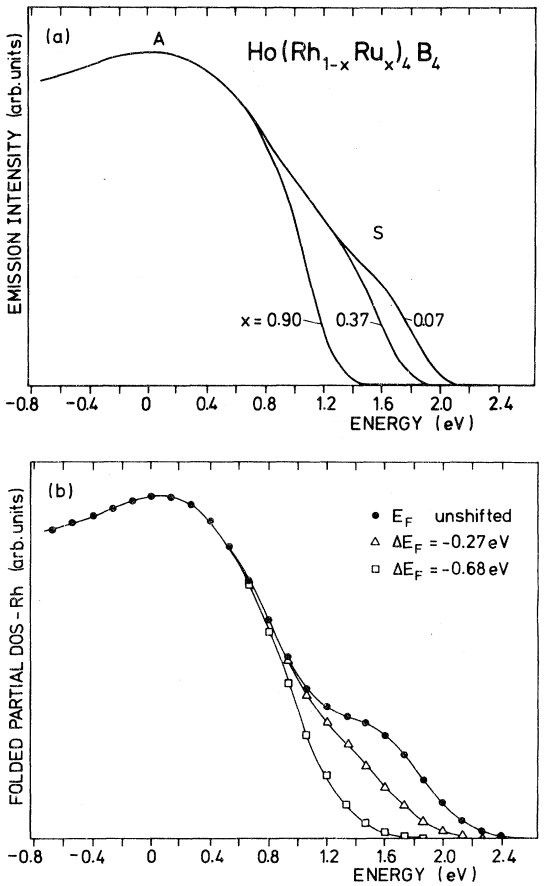

FIG. 6. (a) Photoemission spectra of the Fermi edge of $Ho(Rh_{1-x}Ru_x)_4B_4$ for $h\nu=60$ eV. All spectra are normalized and aligned to peak A. The labels A and S correspond to those in Fig. 2. (b) Calculated partial d-electron density of states for Rh in $HoRh_4B_4$ broadened by a Gaussian of 0.3-eV width. The position of E_F is successively shifted to lower energies with respect to the calculated position for the sample with $x=0.07$. The symbols correspond to the histogram bars.

best fit to our experimental data. Integrating the calculated partial density of states one expects a shift of two bars (0.27 eV) for $x=0.37$ and six to ten bars (0.88 eV) for $x=0.90$ relative to the position for $x=0.07$. In case of the total density of states the values are 0.14 and 0.68 eV, respectively. The striking resemblance between Figs. 6(a) and 6(b) is evident.

In terms of binding energies E_B, the shift of E_F causes the variation of E_B of feature A given in Table I. If a rigid-band model were true the binding energies of the Ho $4f$ states should, of course, change in the same way. However, as can be seen from Table I, this is not the case. The binding energies of features B and C remain nearly constant within the experimental error. The fact that the energy differences between features A and B, as well as A and C, increase upon reducing the number of d electrons, clearly shows the failure of a rigid-band model. As it is a reasonable assumption that the localized Ho $4f$ states are not influenced by the substitution, one has to conclude that the center of the d-band structure is shifted to higher energies. This effect cancels the observed shift of the shoulder of feature A. Such a variation of the energy of a band with occupation is not extraordinary. For example, in case of the Chevrel-phase cluster compounds $M\mathrm{Mo_6S_8}$, a variation of the third element M leads to a change of the number of valence electrons per $\mathrm{Mo_6S_8}$ cluster due to different charge transfers. Nohl *et al.*[24] showed in detailed band-structure calculations that this influences position and dispersion of the electronic bands.

In order to calculate the behavior of T_c from the observed shift of E_F relative to the d-band structure, one needs to know $N(E)$ in detail. In the existing band-structure calculation E_F is shifted through two histogram bars of almost equal height (4.4 and 4.5 states/eV cell spin) if x increases from 0.07 to 0.37. This is consistent with a nearly constant T_c. With further increasing x, E_F moves into the region of low $N(E)$. The resulting drop of $N(E_F)$ provides a straightforward explanation of the observed behavior of T_c. A further shift of E_F caused by x values near 1 should again bring E_F into a region of high $N(E)$. For the nonmagnetic $\mathrm{YRu_4B_4}$ and $\mathrm{LuRu_4B_4}$ compounds superconductivity was indeed observed.[6,9,11] It is conceivable that the different characters of the d bands situated at E_F for $x\approx 1$ also change the sign of the exchange interaction leading to ferromagnetism. This may be the reason that the phase diagrams of the magnetic systems show ferromagnetism instead of superconductivity for high values of x. However, it is not clear to what extent this explanation of the $\mathrm{Ho(Rh_{1-x}Ru_x)_4B_4}$ phase diagram is valid for pseudoternary systems in which the valence-electron concentration is not changed.

V. CONCLUSIONS

With the use of synchrotron radiation, the variation of the photon energy allowed a dependable identification of the different contributions in the measured valence-band spectra. In agreement with band-structure calculations for the primitive-tetragonal modification the analysis shows that the transition-metal d-electron states are dominant near E_F. In order to explain our results it is not necessary to postulate sophisticated mechanisms. The substitution of Ru for Rh reduces the number of d electrons, and one would therefore expect a shift of E_F relative to the d-band structure which, according to our data, indeed occurs. Combined with the particular energy dependence of the d-electron density of states, this shift in E_F leads to a variation of $N(E_F)$ which qualitatively accounts for the peculiar superconducting phase diagram. However, this explanation should not be valid for the completely analogous behavior in T_c when Ir is substituted for Rh, because the number of d electrons is not changed. To clarify this point photoemission measurements of the system $\mathrm{Ho(Rh_{1-x}Ir_x)_4B_4}$ are in preparation.

ACKNOWLEDGMENTS

We would like to thank the staff of Hamburger Synchrotronstrahlungslabor (HASYLAB) for their technical assistance during the photoemission measurements. In particular, one of us (R.K.) thanks the members of Professor Manuel Cardona's group at the Max-Planck-Institut für Festkörperforschung, Stuttgart, for their hospitality. Part of this work was supported by the Bundesministerium für Forschung und Technologie.

[1] *Proceedings of the International Conference on Ternary Superconductors,* edited by G. K. Shenoy and F. Y. Fradin (Elsevier, New York, 1981).

[2] Ø. Fischer, A. Treyvaud, R. Chevrel, and M. Sergent, Solid State Commun. 17, 21 (1975).

[3] R. N. Shelton, R. W. McCallum, and H. Adrian, Phys. Lett. 76A, 213 (1976).

[4] B. T. Matthias, E. Corenzwit, J. M. Vandenberg, and H. Barz, Proc. Nat. Acad. Sci. U.S.A. 74, 1334 (1977).

[5] W. A. Fertig, D. C. Johnston, L. E. DeLong, R. W. McCallum, M. B. Maple, and B. T. Matthias, Phys. Rev. Lett. 38, 987 (1977).

[6] D. C. Johnston, Solid State Commun. 24, 699 (1977).

[7] H. E. Horng, and R. N. Shelton, in *Proceedings of the International Conference Ternary Superconductors,* Ref. 1, p. 213.

[8] H. C. Hamaker and M. B. Maple, in *Proceedings of the International Conference on Ternary Superconductors,* Ref. 1, p. 201. H. C. Hamaker, and M. B. Maple, J. Low Temp. Phys. 51, 633 (1983).

[9] H. E. Horng, Ph.D. thesis, Iowa State University, 1982.

[10] D. C. Johnston, Solid State Commun. 42, 453 (1982).

[11] R. N. Shelton, H. E. Horng, A. J. Bevolo, J. W. Richardson, R. A. Jacobson, S. D. Bader, and H. C. Hamaker, Phys. Rev. B 27, 6703 (1983).

[12] H. C. Ku and F. Acker, and B. T. Matthias, Phys. Lett. 76A, 399 (1980).

[13] H. C. Ku and F. Acker, Solid State Commun. 35, 937 (1980).

[14] H. C. Ku, B. T. Matthias, and H. Barz, Solid State Commun.

32, 937 (1979).
[15]H. C. Hamaker, G. Zajac, and S. D. Bader, Phys. Rev. B 27, 6713 (1983).
[16]T. Jarlborg, A. J. Freeman, and T. J. Watson-Yang, Phys. Rev. Lett. 39, 1032 (1977).
[17]Y. Muto, H. Jwasaki, T. Sasaki, N. Kobayashi, M. Jkebe and M. Isino, in *Proceedings of the International Conference on Ternary Superconductors,* Ref. 1, p. 197.
[18]H. Iwasaki, M. Isino, and Y. Muto, Physica 108B, 759 (1981).
[19]*Synchrotron Radiation: Techniques and Applications,* edited by C. Kunz (Springer, Berlin, 1978).
[20]F. Gerken, Hamburger Synchrotronstrahlungslabor Interner Bericht DESY-F41, HASYLAB 83-03, Hamburg, 1983 (unpublished).
[21]*Photoemission in Solids II,* edited by L. Ley and M. Cardona (Springer, Berlin, 1979), pp. 373ff.
[22]A. J. Freeman and T. Jarlborg, in *Superconductivity in Ternary Compounds II,* edited by M. B. Maple (Springer, Berlin, 1982), pp. 167ff.
[23]J. H. Weaver, C. Krafka, D. W. Lynch, and E. E. Koch, in *Physics Data* (ZAD, Karlsruhe, 1981), Vol. 18-2.
[24]H. Nohl, W. Klose, O. K. Andersen, in *Superconductivity in Ternary Compounds I,* edited by Ø. Fischer and M. B. Maple (Springer, Berlin, 1982), pp. 165ff.